Detection of Winding Asymmetries in Wound-Rotor Induction Motors via Transient Analysis of the External Magnetic Field

Israel Zamudio-Ramirez, Jose A Antonino-Daviu, Roque A. Osornio-Rios, Rene de J. Romero-Troncoso, Hubert Razik

Abstract—Over recent decades, the detection of faults in induction motors has been mainly focused in cage motors due to their extensive use. However, in recent years wound-rotor motors have received special attention because of their broad use as generators in wind turbine units as well as in some large power applications in industrial plants. Some classical approaches perform the detection of certain faults based on the FFT analysis of the steady state current (MCSA); they have been lately complemented with new transient time-frequency-based techniques to avoid false alarms. Nonetheless, there is still a need to improve the already existing methods to overcome some of their remaining drawbacks and increase the reliability of the diagnostic. In this regard, emergent technologies are being explored, such as the analysis of stray flux at the vicinity of the motor, which has been proven to be a promising option to diagnose the motor condition. Recently, this technique has been applied to detect broken rotor bar failures and misalignments in cage motors, offering the advantage of being a non-invasive tool with simple implementation and even avoiding some drawbacks of well-established tools. However, the application of these techniques to wound rotor induction motors (WRIM) has not been studied. This work explores the analysis of the external magnetic field under the starting to detect rotor winding asymmetry defects in WRIM by using advanced signal processing techniques. Moreover, a new fault indicator based on this quantity is introduced, comparing different levels of fault and demonstrating the potential of this technique to quantify and monitor rotor winding asymmetries in WRIM.

Index Terms—Stray flux, time-frequency transforms, transient analysis, wound rotor induction motor.

I. Introduction

DUE to their robustness, simplicity and reliability, induction motors (IM) have been widely used as electromechanical devices for energy conversion [1]. Among the IM types, squirrel-cage and wound-rotor are the most common, this latter being less employed, but with some advantageous characteristics over other types of motors. In this regard, they are able to develop high start torques at lower start-up currents, making them adequate for industrial applications such as ball and sag mills, cranes, pumps, fans and blowers, conveyors, chippers or hoists [2-3]. Recently, they have been massively used as generators in wind turbine units. One of the drawbacks of the wound rotor induction motors (WRIM) in comparison with their cage rotor counterparts is their more delicate maintenance due to the more complex configuration of the rotor circuit which implies the use of slip ring/ brushes systems to access to the rotor winding. These systems are prone to suffer different types of failures due to defective contacts between slip ring and brushes, uneven wear of the brushes in the three phases, high-resistive joints and inadequate or uneven tightening of the springs. Indeed, some studies have shown that most failures of electric motors can be attributed to the bearings and windings [4]. Rotor winding asymmetries can lead to very negative consequences causing unbalanced systems of rotor currents with subsequent parasitic torques and can also cause excessive vibrations and high energy dissipations [5]. These can lead to abnormal motor operation and even to irreparable insulation damages, causing notable losses for the involved companies [6]. Hence, an early detection of rotor asymmetries is of paramount importance for assuring their continuous operation in the applications where these machines are involved.

The detection of some of the previous faults in WRIM has been mainly based on methodologies that rely on the analysis of electrical signals. One of the most recurrent techniques is the well-known spectral analysis of the steady state current using the Fourier transform (Motor Current Signature Analysis, MCSA); the idea is to evaluate the amplitude of the amplified components in case of failure [7-10]. Other works in the literature have proposed alternative methodologies by analyzing vibration signals [11], or other quantities such as speed and current [12] to diagnose failures in WRIM. Even though some of these techniques have shown prominent results, they have similar drawbacks as those arising when they are applied to cage motors. For instance, they are not immune to false indications caused by the presence of load torque oscillations or supply voltage fluctuations [13-15]. Due to these problems, some authors have proposed to combine different physical variables for reaching a more accurate diagnostic conclusion. In this regard, combinations as vibration/torque or stray magnetic field/vibration have been suggested [16-17].

Recently, several authors have developed alternative techniques that rely on the analysis of starting currents using more sophisticated Time-Frequency Decomposition (TFD)

I. Zamudio-Ramirez, R.A Osornio-Rios and R.de J. Romero-Troncoso are with the CA Mecatronica, Facultad de Ingenieria, Campus San Juan del Rio, Universidad Autonoma de Queretaro, San Juan del Rio 76807, Queretaro, MEXICO, (e-mails: isra.zam.ram@hotmail.com, raosornio@hspdigital.org, troncoso@hspdigital.org).

J. Antonino-Daviu is with the Instituto Tecnológico de la Energía, Universitat Politècnica de València, Valencia, SPAIN (e-mail: joanda@die.upv.es)

H. Razik is with Université de Lyon, Ampère, CNRS UMR 5005, Ecole Centrale de Lyon, INSA-Lyon, UCB Lyon 1, F-69100, Villeurbanne, FRANCE (e-mail: Hubert.razik@univ-lyon1.fr) .

tools. The underlying idea is to detect evolutions of fault-related components that occur under the starting. In this context, [18-21] propose the use of discrete wavelet transforms (DWT) to detect diverse faults in WRIM. Wigner-Ville Distribution was proposed in [22] to sense the high-frequency rotor failure harmonics, while [23] presented a combination of procedures, first the Empirical Mode Decomposition (EMD) method to track the low frequency fault-related components and then the Wigner-Ville Distribution at the startup of the motor. Finally, [10] suggests the analysis of the starting current using the DWT and the Short Time Fourier Transform to obtain diverse evidences of rotor asymmetries in WRIM. All these approaches, based on the transient analysis of motor currents, improve the reliability of the diagnosis advantaged by the ability of these techniques to detect evolutions of fault-related components, which are very reliable evidences of the presence of the fault and which are much more conclusive than detecting a single peak in the FFT spectrum. However, they cannot avoid some of the problems derived from the use of current signals for fault diagnosis purposes.

The interesting advantages provided by the techniques based on motor currents analysis (both at steady-state and at transient regime) do not imply that investigation in alternative techniques based on other quantities is useless. In this regard, the study of the magnetic field on the vicinity of the motor is recently drawing the attention of many researchers [24-28]. This is especially due to advantages such as the simplicity of the technique and its non-invasive nature, as well as the spectacular cost reduction of the necessary sensors that has come together with significant advances in their features (reduced volumes, high accuracy in the data acquisition and easy portability) [29]. These facts have conferred an interesting potential to the technique for complementing the diagnosis provided by other quantities, in cases where these cannot be easily measured or where they do not lead to conclusive diagnostics. In this regard, it has been recently proven that flux data analysis helps to avoid false indications provoked by the presence of rotor cooling ducts which may occur if classical current or vibration methods are used [30].

Nonetheless, the knowledge about the stray flux analysis technique is still much more limited in comparison with others. In this regard, most of the few available works have been focused on the study of stationary flux signals by applying classical Fourier transforms [24-27]. In contrast, the application of the technique under transient conditions has been barely exploited, although very recent works have proven the potential of this analysis for detecting rotor failures and eccentricities [28], being all the previous works dedicated to cage motors.

The present work introduces a novel methodology for the detection, monitoring and quantification of rotor winding asymmetry defects in WRIM. To this end, the analysis of transient stray-flux signals under starting is proposed. Short-time Fourier Transform (STFT) and DWT are applied in this work to track the corresponding fault components in the transient flux signals. Three different flux sensors positions

are considered in the study; the components amplified in each case are studied and justified. Moreover, given the importance of the classification of the failure in the automation of the diagnosis process, a fault level indicator is defined based on the flux transient time-frequency obtained results.

II. TRANSIENT ANALYSIS OF THE EXTERNAL MAGNETIC FIELD

The effectiveness of the analysis of the external magnetic field applied to induction motors has been verified and validated in different works [24-28], in which failures such as shorted turns in stator winding, broken rotor bars, static and dynamic rotor eccentricity, and bearing faults are efficiently detected by suitable signal processing techniques. Regarding rotor asymmetry failures in WRIM, it has been demonstrated in some works such as [35] (which applies the Fortescue's theorem to the unbalanced system of rotor currents created by a winding asymmetry) that specific frequency components are amplified both in the flux and current signals in case of failure. The most significant components amplified by the asymmetry are given by (1), which corresponds to the frequencies of the main sideband components around the fundamental [31]:

$$f_{raS}(s) = (1 \pm 2 \cdot s) \cdot f \qquad (1)$$

where f_{raS} are the frequencies of the fault-related components, f is the supply frequency and s is the slip.

On the other hand, other recent works applied to cage motors have proven that, in case of rotor asymmetries, additional components given by $s \cdot f$ and $3 \cdot s \cdot f$ are amplified in the FFT spectrum of the stray flux signals [24]. These components have an axial nature and, therefore, they are more likely detected at those sensor positions in which a higher portion of axial flux is captured. The amplitude of the component at $s \cdot f$ can be also incremented by the presence of eccentricity/misalignment [24, 28]. One of the objectives of this work is to verify if these axial components are also amplified in case of rotor asymmetries in WRIM.

Conventional methods relying on stray-flux analysis detect the aforementioned components in cage induction motors but using steady-state flux signals which are analyzed through the Fourier transform. On the contrary, this work proposes, for the first time, the analysis of these signals under starting to detect rotor asymmetries in WRIM. In the case of a direct-on-line starting, the variation of the slip s during the motor starting will lead to particular trajectories of the abovementioned slip-dependent flux components, developing in a characteristic way according to slip changes. Therefore, the application of suitable time-frequency transforms (such as the DWT or STFT, the suitability of which was widely proven in previous works) to the electromotive force signals induced by the magnetic field in external coil sensors under starting will enable to visualize those trajectories, which will become reliable evidences of the presence of the asymmetry.

In the present work, the coil flux sensor is installed in the vicinity of the motor frame at three different positions to measure the axial and radial flux components according to the

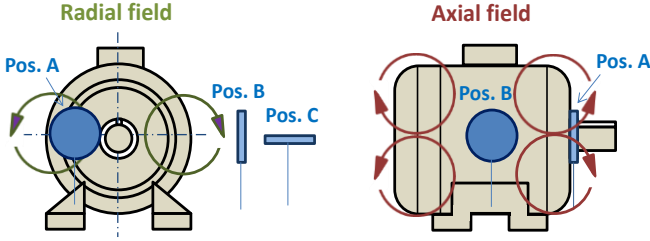placement thereof. Thus, in Fig. 1 are shown the positions A, B, and C in which the sensor is installed.

Fig. 1. Coil sensor positions in tested WRIM.

In position A, the sensor mainly measures the axial flux; on the other hand, if the sensor is placed in position B the result of the measurements will correspond to components of axial flux and part of radial flux simultaneously, while the position C measures radial flux essentially.

To identify the severity of the failure, an indicator analogue to that suggested in previous works for the detection of rotor problems in cage motors but adapted here to detect asymmetries in WRIM [28, 33] is used. This normalized indicator (γ_{DWT}), given by (2), relies on the fact that energies of the faulty band wavelet component increase as the fault severity does and for the case in which a magnetic field is monitored, it relates the electromotive force (emf) induced in the coil sensor with that of the wavelet signal containing most of the fault component evolution (d_n).

$$\gamma_{DWT}(dB) = 10 \cdot \log \left[\frac{\sum\limits_{j=Nb}^{N_s} emf_j^2}{\sum\limits_{j=Nb}^{N_s} [d_n(j)]^2} \right] \quad (2)$$

where N_s is the number of samples of the signal until the fault-related oscillations disappear in the wavelet signal and N_b indicates the sample number at the origin of the considered time interval.

III. RESULTS AND DISCUSSION

The diagnostic procedure proposed in this paper was validated in the laboratory on a 4P, 400V, 11kW WRIM. The rotor windings were allocated in 24 slots and the resistance per phase was 0.335 Ω [35]. Several experiments were carried out both for the motor in healthy conditions and for the motor having up to four levels of induced rotor asymmetries.

A. Experimental setup.

The level of failure induced in the motor was controlled using an external rheostat inserted in series with one of the rotor windings; different levels of rotor asymmetry were achieved by varying the resistance of this rheostat. The rheostat was a variable resistor with 10 levels of resistance that were selectable by the user. The maximum phase-to-phase resistance level was 11.6 Ω (step 10) and the minimum 0.14 Ω (step 1). Furthermore, to obtain the axial and radial flux components, a flux sensor was installed in the motor frame at the three positions A, B, and C showed in Fig.1. The flux sensor was a coil with 1000 turns with an external diameter of 80mm and an internal diameter of 39mm. The corresponding

induced emf signals were captured under starting and at steady-state by connecting the coil sensor to a digital waveform recorder where the measured data were stored. A sampling rate $f_s = 5\ kHz$, and an acquisition time of 60s was set, which was enough to capture the transient and the steady-state of the motor. Figure 2 shows the tested WRIM, the signal acquisition system, the external rheostat and one of the considered flux coil sensor positions (Pos. B).

The experiments were developed under different load levels (no load, partial load and full load). The no load condition is a more critical situation for detecting the fault related components in the flux signals, due to the reduced value of the slip s. Under this condition, the classical steady-state methods may have difficulties for detecting the $f \cdot (1 \pm 2 \cdot s)$ components since these may overlap with the supply frequency f due to the low slip value The proposed starting transient based method avoids this problem, since the fault patterns are clearly present under starting regardless of the load level.
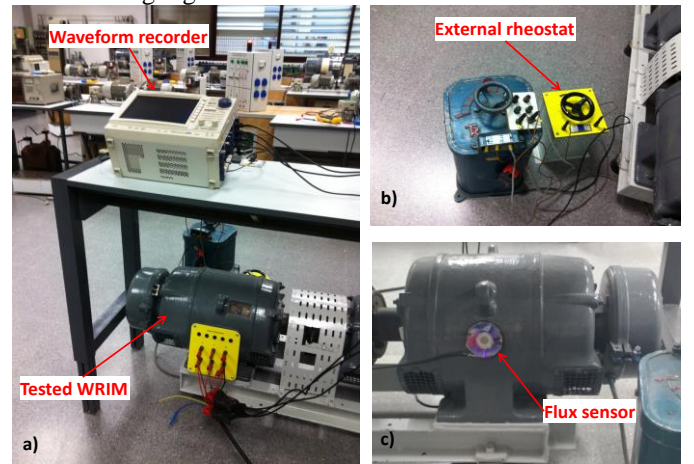

Fig. 2. Laboratory test bench: a) Waveform recorder and tested WRIM, b) external rheostat for forcing the asymmetries and c) flux sensor at position B.

B. Data analysis.

To perform the analysis of the corresponding emf signals, the measured data are transferred to a computer where suitable digital signal processing techniques are applied. Because the study presented here is focused on a specific frequency band below 150 Hz, the signal of interest is filtered by a fourth order Butterworth filter with a cut-off frequency of 150 Hz.

Then, for the time-frequency analyses, two different tools were applied to the different coil sensor emf signals captured and stored during transient. On the one hand, the STFT is used to track fault components evolutions under starting. In healthy conditions, only the fundamental component (FC) is expected to be present; it should appear as a horizontal line at the supply frequency (50 Hz). Under the presence of rotor asymmetry, the FC is expected to be accompanied by the characteristic t-f patterns caused by the evolutions of the fault components. The second signal processing technique used is the DWT. This technique is selected for its ability to decompose a signal into well-defined 'wavelet signals' that cover specific frequency ranges, known to be directly dependent on the sampling frequency used to capture the analysed signals [34]. In addition, there are algorithms that

facilitate its application and improve its performance, processing time, and computational burden that entails its application. In this regard, the proposed indicator expressed by (2) is based on the energy of one of these wavelet signals. A good election of the wavelet signal is essential for the diagnosis to be reliable, so this wavelet signal must cover part of the frequency band through which the considered fault component (we will focus on $(f \cdot (1-2s))$) evolves under starting, in such a way that it is possible to capture the changes of energy levels that arise when the fault occurs, since these harmonics disappear together with the fault.

For this purpose, Fig. 3 shows the DWT analyses of the *emf* signals induced in the coil sensor at positions A, B, and C under motor starting (db44 was used as mother wavelet for the analyses) and compares the cases when the motor is in healthy condition (left hand side of Fig. 3) against those of the motor with the presence of asymmetry in the rotor (right hand side of Fig. 3). The upper waveform (in red color) is the analyzed *emf* signal. The waveforms showed below correspond to the wavelet signals that are more relevant for the outlined purposes of this paper, namely: d_6, d_7, d_8 and a_8.

It is noteworthy that the signals d_7, d_8 and a_8 have very low oscillations amplitudes when the motor is healthy. On the other hand, when the motor has the presence of rotor asymmetry failures, very clear oscillations with higher amplitudes appear in signals d_7, d_8 and a_8 (see right hand side of Fig. 3). This is mainly attributed to the fact that the energy of these signals is affected for the time evolution of the $f \cdot (1-2s)$ component created by the rotor fault under starting, in such a way that when the motor is connected and it starts to accelerate the fault component starts to appear at the FC (signal d_6), then it evolves through signals d_7, d_8 and a_8 that cover the frequency bands below 50 Hz following an specific pattern until the slip is approximately zero, as marked in the corresponding graphs by the red arrows (note that there also other minor oscillations in these signals caused by the evolutions of other fault related components (e.g. at $s \cdot f$)).

Considering this, we propose to use the wavelet signal d_8, which covers the frequency range ~ [10Hz-20Hz], because the sampling frequency used is 5 kHz, so that part of the aforementioned and desired frequency band is covered.

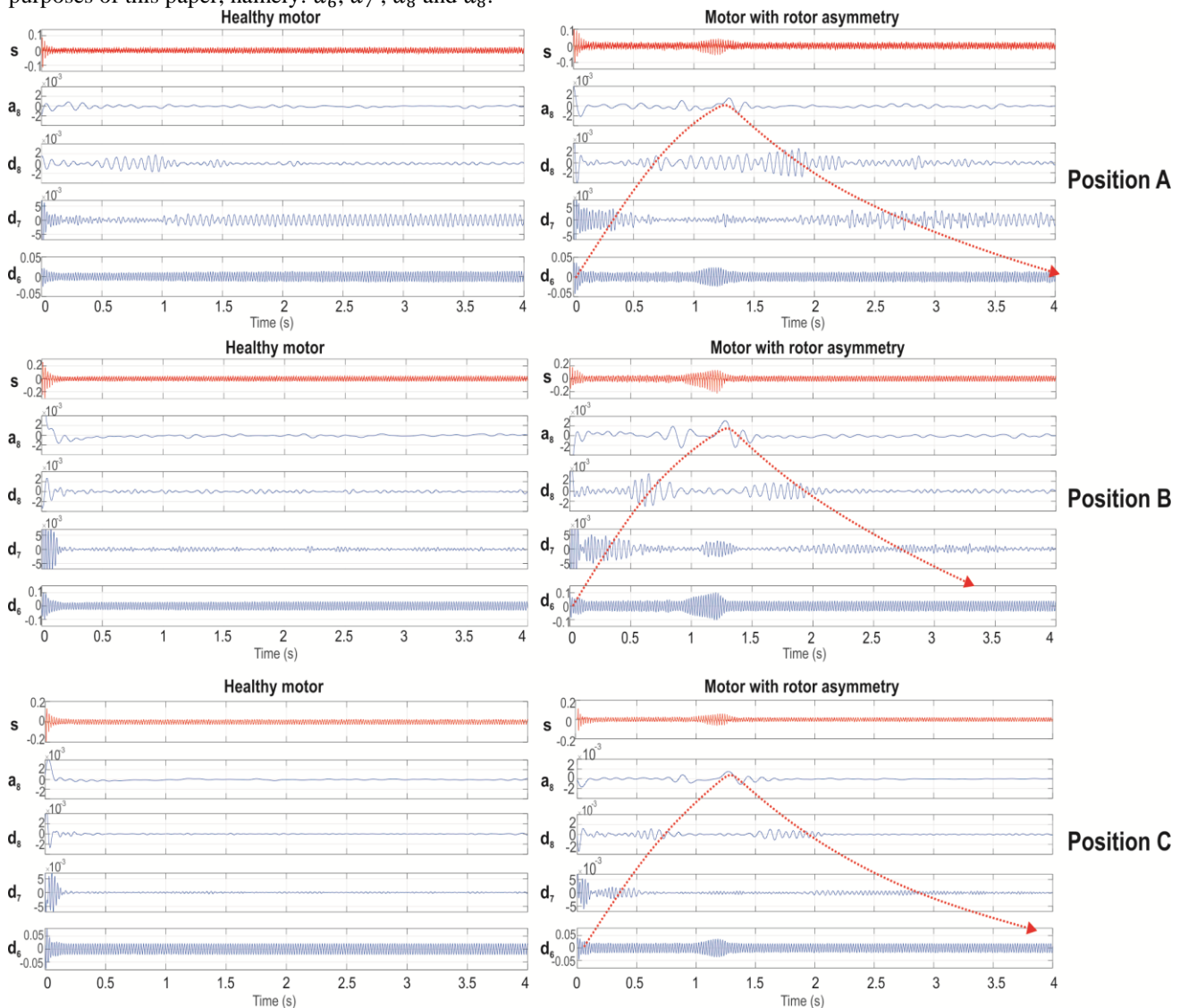

Fig. 3. DWT analysis of the emf signal under starting (red signal) with the sensor at the three different positions studied here for a healthy motor (left hand side) and motor with rotor asymmetry (right hand side).

Figure 4 illustrates the differences in the amplitudes of the oscillations that appear in the signal d_8, for the sensor placed in position B. Note that, the greater the severity of the failure is, the higher the amplitude of these oscillations, demonstrating that the energy of these signals is affected by rotor asymmetry faults in WRIM. In the same figure, it is highlighted in red those areas that are used for the calculation of the flux indicator γ_{DWT}, such areas correspond precisely to the time interval in which the evolution of the fault penetrates the signal d_8.
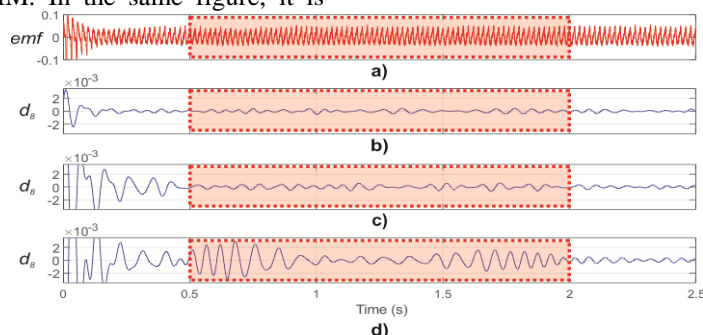

Fig. 4. DWT analysis of the emf signal when the sensor is placed in position B: (a) total emf signal under starting, (b) signal d_8 for a healthy motor, (c) d_8 signal for a motor with rotor asymmetry level two, (d) d_8 signal for a motor with rotor asymmetry level four.

On the other hand, Fig. 5 shows the analyzes of the coil sensor signals in the three positions (A, B, and C) using the STFT when the motor has rotor asymmetry faults. This tool enables a clearer visualization of the content of the t-f map. In this regard, note the appearance of the fault components characterized by (1): on the one hand, the component $(1 + 2s)f$ which starts from a frequency of 150 Hz and decreases until approaching the fundamental frequency and, on the other hand, the fault component $(1 - 2s)f$ which evolves following the V-shaped pattern commented before. Note also the presence of the aforementioned component at $s \cdot f$, with axial nature, that is also amplified by the rotor asymmetry. Finally, it is also detected the evolution of a component (f_{ecc}) that is due to the presence of a certain level of misalignment between motor and load and that is present in all the tests. This component is given by $f_{ecc}=f\text{-}f_r$ and evolves from the fundamental frequency (f=50 Hz) to near $f/2$ since the tested machine has two pole pairs [28].
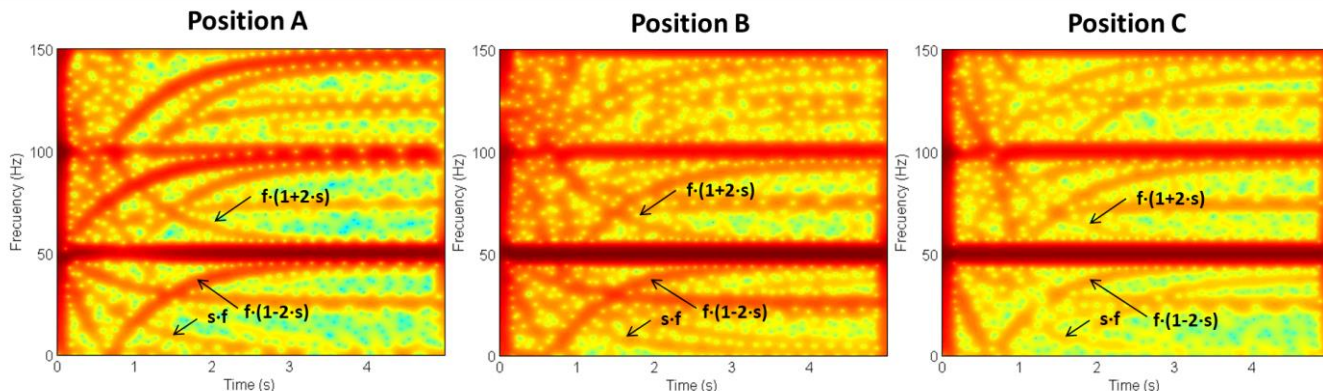

Fig. 5. STFT analyses of the starting coil sensor signals for the machine with rotor asymmetry and for the three positions of the sensor (the color denotes the energy density in each point of the time-frequency map, with red indicating the highest density and blue the lowest density).

Fig. 6 shows the time-frequency analyses using the STFT of the transient *emf* signals in three different tested conditions of the motor, corresponding to the motor in a healthy condition, with a failure severity level two (added resistance R_{add}=1.6 R_R with R_R=rotor resistance) and the case in which the motor has a serious fault corresponding to a failure severity level four (added resistance R_{add}=1.9 R_R). The motor operated under no load. Fig. 7 is equivalent to Fig. 6 but for partial load conditions (3/4 of the rated load) and is displayed to show that the results are also valid for the machine under loaded conditions. At first sight, it becomes evident that there are clear differences between the three fault conditions, since more evolutions are visualized as the rotor asymmetry gets worse. In this regard, the fault components at $f \cdot (1\text{-}2 \cdot s)$ (radial) and $s \cdot f$ (axial) are present in all faulty cases, but their higher or lower intensities depend upon the considered sensor position, as it is clearly observed in the figure. More specifically, the following conclusions can be obtained after a careful analysis of the graph:

- With regards to the component at $f \cdot (1\text{-}2 \cdot s)$, its evolution is clearly discernible for every fault condition at each position of the sensor. Moreover, its intensity increases as the rotor winding asymmetry gets worse (it appears with very low intensity in the healthy cases). This indicates that this component is a very good candidate to be used to detect the presence of the

asymmetry and quantify its severity and this is the reason why the indicator proposed in this work relies on this specific component. On the other hand, although this component has a predominantly radial nature [28], its evolution is observed for all sensor positions, probably because of its predominant amplitude and because for every sensor position a certain portion of radial flux was captured.

- On the other hand, the evolution of the axial component at $s \cdot f$ is also clearly observed. This component is more discernible at position A, since at this sensor position the captured flux is mainly axial. Therefore, this component has much more intensity for this sensor position, whereas it has much less intensity for position B and, especially, for position C. On the other hand, note how, for each specific sensor position, despite this component increases its intensity as the fault severity increases, it is clearly observable even in healthy condition. This is due to the fact that, as reported in previous works, the amplitude of the $s \cdot f$ component is also increased by the presence of misalignments /

eccentricities. Since the tested motor was operating under a certain level of misalignment in all the tests, this leads to a certain increment in the amplitude of this component, even for the tests corresponding to the healthy condition of the rotor winding.

- Finally, note the presence of the component f_{ecc} in all the analyses, even for healthy condition of the rotor winding. As commented, this component (that evolves between f and f-f_r (i.e. between 50 Hz and near 25 Hz for our motor) is due to the presence of a certain level of misalignment between the motor and the driven load. The presence of this misalignment was confirmed with additional analyses of the motor current that confirmed the presence of the components at 25 Hz and 75 Hz in the steady-state current spectra. Interestingly, note that the technique is able to clearly detect this component, informing on the presence of this other type of fault in the machine, which confers a great potential for its future extrapolation for the detection of other failures.
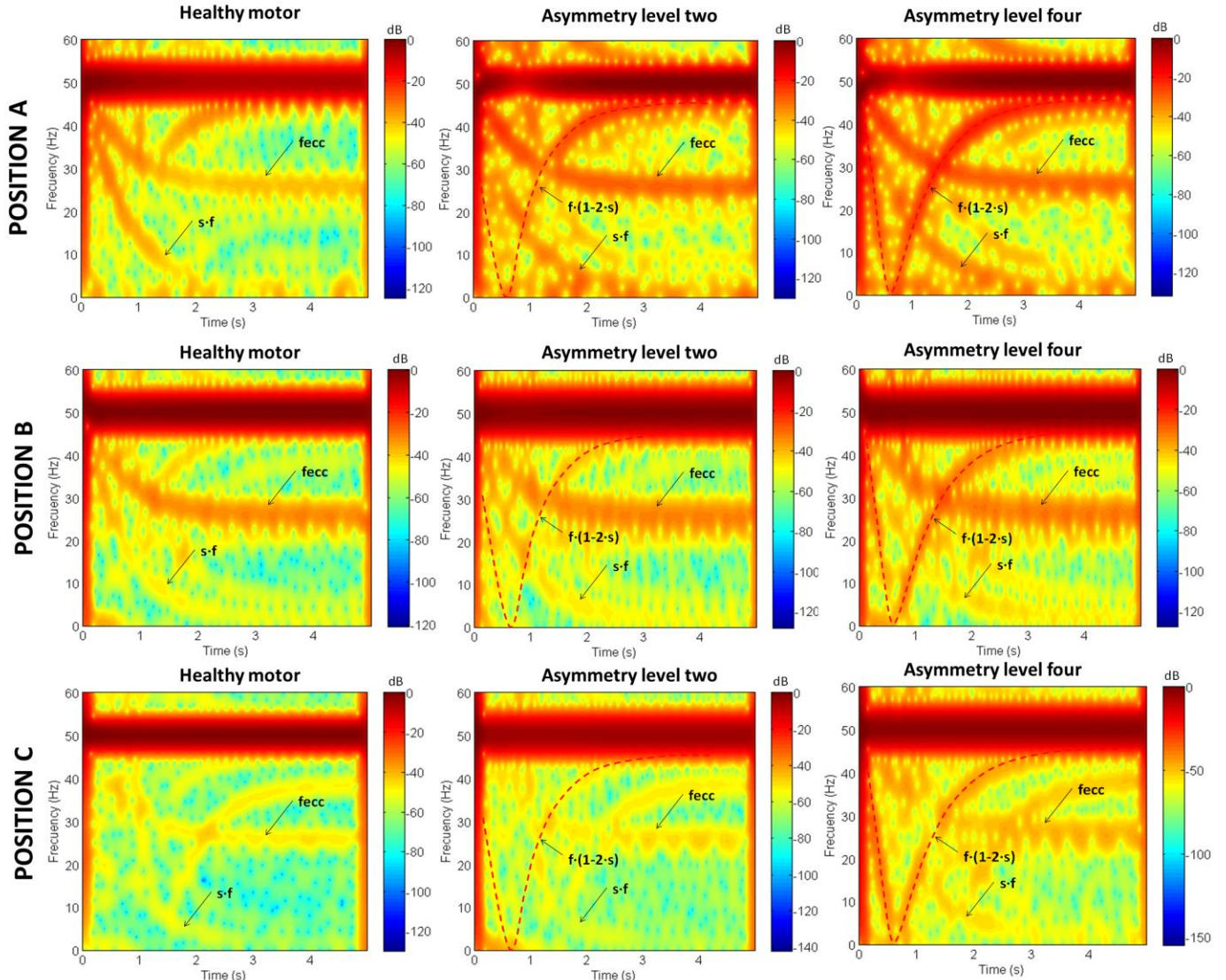

Fig. 6. STFT analyses of the starting coil sensor signals for the motor in healthy state, motor with rotor asymmetry level two out of four and motor with rotor asymmetry level four out of four and for the three considered positions of the sensor (the color denotes the energy density in each point of the time-frequency map, expressed in dB in relative terms versus the fundamental). The motor operates at no load condition.
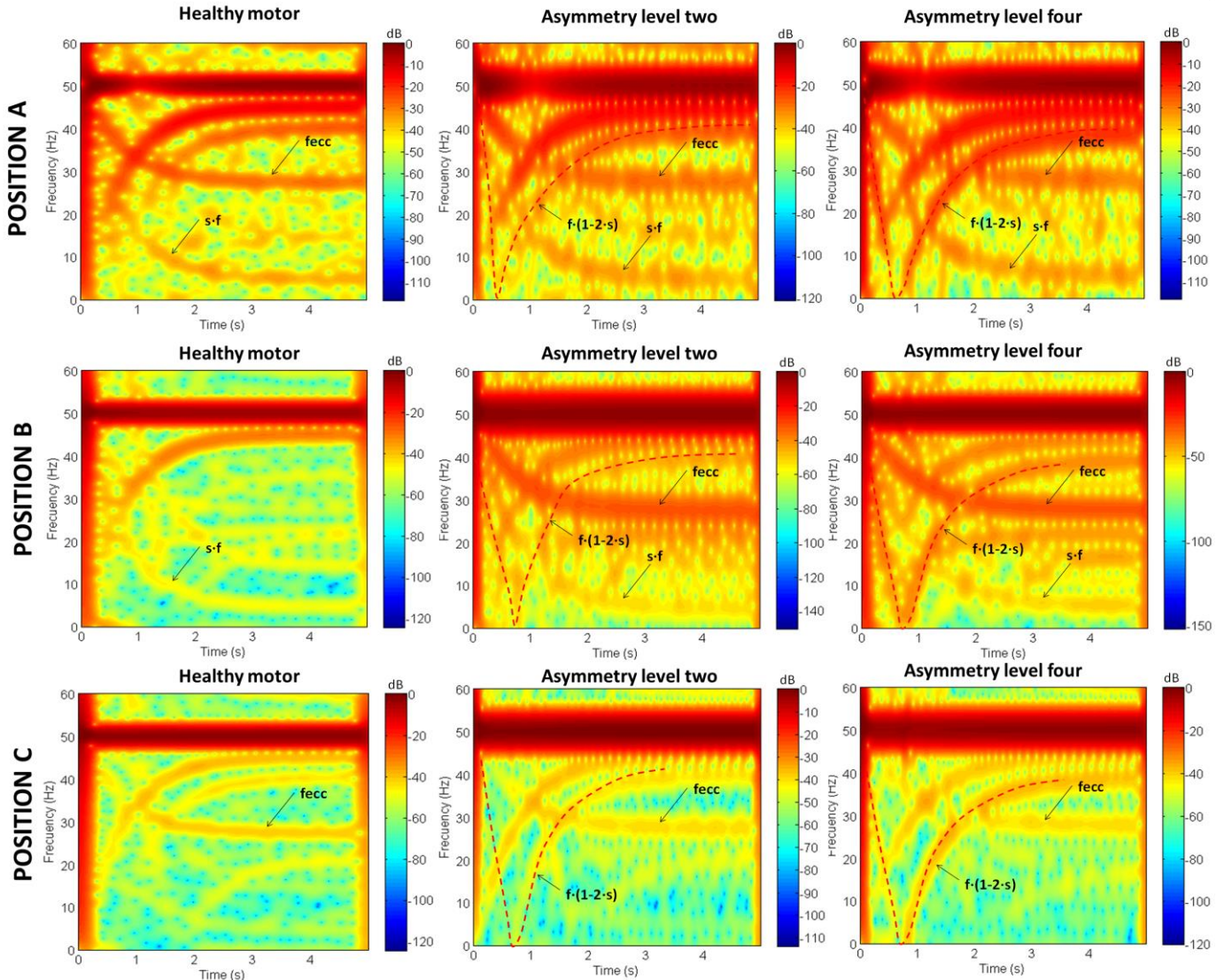
Fig. 7. STFT analyses of the starting coil sensor signals for the motor in healthy state, motor with rotor asymmetry level two out of four and motor with rotor asymmetry level four out of four and for the three considered positions of the sensor (the color denotes the energy density in each point of the time-frequency map, expressed in dB in relative terms versus the fundamental). The motor operates at partial load condition (3/4 rated load).

Furthermore, Fig. 8 shows the results achieved when the flux indicator is computed applying the fault indicator defined by (2) to the wavelet signal d_8 obtained through the DWT. These results are obtained using the sensor coil installed in the three positions A, B, and C according to Fig. 1, and they show that it is possible to detect the severity of rotor asymmetry faults in a WRIM by means of *emf* readings from an external coil sensor attached to the motor. In addition, as it can be seen, the value of the indicator for the case in which the motor is healthy indicates higher levels, while when the severity of the failure becomes increasingly greater, the indicator produces increasingly lower values in dB, following a clear decreasing trend when the level of asymmetry is greater. Indeed, the difference between the motor in healthy condition and the motor with the highest considered fault severity is certainly wide, a fact that demonstrates the effectiveness of the indicator. This situation is attributed to the fact that the considered wavelet signal has low amplitude when the motor is in healthy condition, while its energy begins to increase when the component attributed to the fault appears. Note that at position C, the values are very high compared to A and B positions. This is essentially due to the low amplitude of the fault component; however, the sensitivity is better for the sensor at positions A and B, for every level of rotor asymmetry studied here. Especially, for position B where a higher part of the radial flux is captured. Considering this specific sensor position, a threshold value of the indicator of 35dB could be set for discriminating between healthy and faulty conditions (see Fig. 8).

On the other hand, it is important to mention that it is of vital importance to maintain a fixed coil sensor position, since the results depend on the position in which the sensor is located, and may produce undesirable diagnoses.
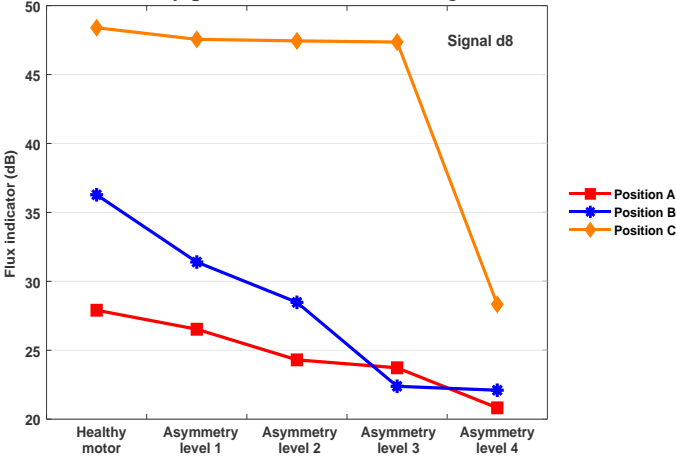

Fig. 8. Values of the γ_{DWT} indicator based on the energy of the d8 wavelet signal, for a healthy motor and for every level of rotor asymmetry induced.

For comparison purposes, Fig. 9 shows the MCSA analyses of the steady-state current for the three considered fault cases. The analyses are referred to a loaded condition since, if the machine is unloaded, the sidebands are difficult to be distinguished due to the reduced slip value. Note that, in all cases, the sideband components caused by the rotor asymmetry are clearly present. These sidebands appear even in healthy condition due to the inherent asymmetry of the rotor winding that is unavoidable in this type of motors due to uneven contacts between the slip-rings and brushes in the three phases, among others. Note that the sidebands' amplitudes increase as the level of rotor winding asymmetry does. However, this increment of the amplitudes is less significant than that obtained with the proposed indicator based on flux analysis under starting. Indeed, for position B of the sensor, the indicator is much more sensitive than that based on MCSA. This would confirm that the method proposed in the paper can be perfectly compared with other approaches and may give better results for some sensor positions.
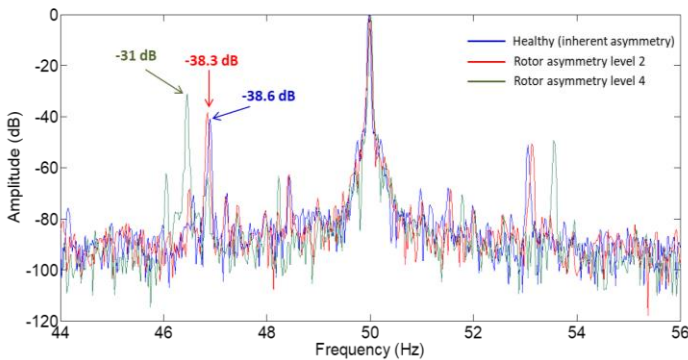

Fig. 9. MCSA analyses of the steady-state current for the considered fault cases

IV. CONCLUSIONS

This work has introduced a new approach to perform the diagnosis of rotor asymmetry faults in WRIM, a type of machine that has been much less studied in the condition monitoring area but that is drawing an increasing attention due to its use in large power applications and as generator in wind turbine generator units. The proposed approach relies on the detection of patterns that appear in the time-frequency maps under motor starting when the fault is present. These patterns are efficiently detected using different signal processing techniques applied to the *emf* signals captured during transient: on the one hand, a continuous tool, the STFT is used to track the evolution of fault harmonics. On the other hand, a discrete transform, the DWT is used as an auxiliary tool in the calculation of a fault severity indicator.

What makes the methodology proposed here even more attractive, is that both tools the STFT and the DWT rely on a non-invasive technique, in which the signals are obtained from an external coil sensor that is attached to the motor frame, and which complies with several characteristics that make it an excellent alternative as a source of information, namely, simple design of the necessary sensor, small size, low cost, and flexibility to be installed anywhere around the electrical machine.

Furthermore, the following conclusions, obtained from the tests under loaded and unloaded conditions, show the relevance and effectiveness of analyzing the stray flux during start to detect asymmetry rotor faults in WRIM:

- The location of the sensor determines the type of components that will be displayed in the t-f space, either axial or radial. However, in all of them there is an evolution of the $f \cdot (1-2 \cdot s)$ failure component under starting that leaves a characteristic V-shaped pattern in case of a rotor asymmetry fault.

- The three sensor positions analyzed here show the appearance and evolution of the failure component at $f \cdot (1+2 \cdot s)$ reported in previous works, where the analyses were performed using current signals, demonstrating that the radial and axial components of the stray flux captured by the coil sensor are sensible to this failure component.

- The fault patterns are detectable even in the case of no load conditions. In this situation, the classical steady-state approaches may fail due to the overlap between the sidebands at $f \cdot (1 \pm 2 \cdot s)$ and the fundamental component at f.

- The component at $s \cdot f$, that is also amplified by the asymmetry, is especially observable at position A, due to its axial nature. However, it is also observed in other sensor positions, since a certain portion of axial flux is captured in each of them.

- The presence of misalignment between the motor and driven load leads to a component f_{ecc} that is clearly discernible in the t-f maps. Its detection confers a great potential to the technique for determining the existence of this fault in the machine. The presence of misalignment also affects the amplitude of the component at $s \cdot f$.

- It is possible to quantify the level of asymmetry by means of the proposed fault severity indicator γ_{DWT} relying on the DWT of the *emf* signals captured under starying. The most sensitive position is position B since a higher portion of flux (axial and radial is captured) at that position. A threshold value of 35 dB has been set for discriminating between healthy and faulty condition for this specific sensor position.

REFERENCES

[1] W.T. Thomson, I. Culbert, *Current Signature Analysis for Condition Monitoring of Cage Induction Motors*, IEEE Press, Wiley, New Jersey, 2017.

[2] H.A. Toliyat, G.B. Kliman, *Handbook of Electric Motors*, CRC Press, 2004.

[3] TECO-Westinghouse Motor Company. *"Wound rotor motor technology"*, Wound rotor motor brochure, http://www.tecowestinghouse.com/PDF/woundrotor.pdf

[4] A. H. Bonnet and C. Yung, "Increased efficiency versus increased reliability," IEEE Industry Applications Magazine, vol.14, no.1, pp.29-36, 2008.

[5] Bellini, A., Filippetti, F., Tassoni, C., Capolino, G.A., "Advances in diagnostic techniques for induction machines*", IEEE Trans. Ind. Electron.*, 55, (12), pp. 4109–4126, 2008.

[6] Barreto G., Jonas, Morales C., Rangel J., Peregrina H., "Half-broken bar detection using MCSA and statistical analysis.", *2017 IEEE International Autumn Meeting on Power, Electronics and Computing (ROPEC)*, pp. 1-5. IEEE, 2017

[7] Stefani, A., Yazidi, A., Rossi, C., Filippetti, F., Casadei, D., Capolino, G.-A., "Doubly fed induction machines diagnosis based on signature analysis of rotor modulating signals", *IEEE Trans. Ind. Appl.*, 2008, 44, (6), pp. 1711–1721.

[8] L. Jun-qing, W. Dong, and H. Long, "Study of rotor winding inter-turn short circuit fault in doubly fed induction generator based on current signal spectrum analysis," *in International Conference on Electrical Machines and Systems (ICEMS)*, Oct 2013, pp. 789–792

[9] S.Williamson, S.Djurović, "Origins of Stator Current Spectra in DFIGs with Winding Faults and Excitation Asymmetries," *Proc. of IEEE IEMDC 2009* Miami, pp. 563-570, May 2009.

[10] J. Antonino-Daviu, A. Quijano-López, V. Climente-Alarcon and C. Garín-Abellán, "Reliable Detection of Rotor Winding Asymmetries in Wound Rotor Induction Motors via Integral Current Analysis," in *IEEE Transactions on Industry Applications*, vol. 53, no. 3, pp. 2040-2048, May-June 2017.

[11] N. Sarma, Q. Li, S. Djurovic, A. C. Smith and S. M. Rowland, "Analysis of a wound rotor induction machine low frequency vibroacoustic emissions under stator winding fault conditions," *8th IET International Conference on Power Electronics, Machines and Drives (*PEMD 2016), Glasgow, 2016, pp. 1-6.

[12] D. E. Khodja and B. Chetate, "Torque based selection of ANN for fault diagnosis of wound rotor asynchronous motor-converter association," *National Conference on Electrical, Electronics and Computer Engineering*, Bursa, 2010, pp. 339-343.

[13] A. Stefani, F. Filippetti, and A. Bellini, "Diagnosis of induction machines in time-varying conditions," in *Proc. IEEE Int. SDEMPED*, Cracow, Poland, Sep. 2007, pp. 126–131

[14] J. Y. Gritli, C. Rossi, 1. Zarri, F. Filippetti, A. Chatti, D. Casadei, "Double Frequency Sliding and Wavelet Analysis for Rotor Fault Diagnosis in Induction Motors under Time-Varying Operating Condition" *8th IEEE-SDEMPED' I* I, Bologna, Italy 2011.

[15] J. Cusido, L. Romeral, J.A. Ortega, A. Garcia, J.R. Riba, "Wavelet and PDD as fault detection techniques" *Electr. Power Syst. Re*s., 80 (2010), pp. 915-924.

[16] M. Cuevas, R. Romary, J.-P. Lecointe, and T. Jacq, "Non-invasive detection of rotor short-circuit fault in synchronous machines by analysis of stray magnetic field and frame vibrations," *IEEE Transactions on Magnetics*, vol. 52, no. 7, pp. 1–4, 2016.

[17] S. Djurovic, D. Vichis-Rodriguez, and AC., Smith, "Investigation of wound rotor induction machine vibration signal under stator electrical fault conditions," *The lET Journal of Engineering*, pp. I-II, May 2014

[18] J. Gritli, Y., Zarri, L., Rossi, C., et al., "Advanced diagnosis of electrical faults in wound-rotor induction machines", *IEEE Trans. Ind. Electron.*, 2013, 60, (9), pp. 4012–4024.

[19] J G. Niu, A. Widodo, J. Son, B. Yang, D. Hwang, D. Kang, "Decision-level fusion based on wavelet decomposition for induction motor fault diagnosis using transient current signal". *Expert Syst. Appl.*, 35 (2008), pp. 918-928.

[20] J. Y. Gritli, A. Stefani, C. Rossi, F. Filippetti, A. Chatti, "Experimental validation of doubly fed induction machine electrical faults diagnosis under time-varying conditions". *Electr. Power Syst. Res.*, 81 (3) (2011), pp. 751-766.

[21] M. Keravand, J. Faiz, M. Soleimani, M. Ghasemi-Bijan, M. BandarAbadi and S. M. Â. Cruz, "A fast, precise and low cost stator inter-turn fault diagnosis technique for wound rotor induction motors based on wavelet transform of rotor current," *2017 IEEE 11th International Symposium on Diagnostics for Electrical Machines, Power Electronics and Drives (SDEMPED)*, Tinos, 2017, pp. 254-259.

[22] V. Climente-Alarcon, M. Riera-Guasp, J. Antonino-Daviu, J. Roger-Folch, and F. Vedreno-Santos, "Diagnosis of rotor asymmetries in wound rotor induction generators operating under varying load conditions via the Wigner-Ville Distribution," in *Proc. SPEEDAM*, pp. 1378–1383, 2012.

[23] J. Antonino-Daviu, V. Climente-Alarcon, I. Tsoumas, G. Georgoulas and R. B. Pérez, "Multi-harmonic tracking for diagnosis of rotor asymmetries in wound rotor induction motors," *Industrial Electronics Society, IECON 2013 - 39th Annual Conference of the IEEE*, Vienna, 2013, pp. 5555-5560.

[24] A. Ceban, R. Pusca and R. Romary, "Study of Rotor Faults in Induction Motors Using External Magnetic Field Analysis*", IEEE Trans. Ind. Electronics*, vol. 59, no. 5, pp. 2082-2093, 2012.

[25] H.Henao, C.Demian, G.A.Capolino, "A Frequency Domain Detection of Faults In Induction Machines Using an External Flux Sensor", *IEEE Trans. Ind. Appl.*, Vol.39, No.5, Sept./Oct.2003, pp.1272-1279.

[26] Frosini, L., Harlisca, C., Szabó, L., "Induction machine bearing faults detection by means of statistical processing of the stray flux measurement", *IEEE Trans. Ind. Electron.*, 2015, 62, (3), pp. 1846–1854.

[27] R. Romary et al. "Electrical Machines Fault Diagnosis by Stray Flux Analysis" *2013 IEEE Workshop on Electrical Machines Design, Control and Diagnosis (WEMDCD)*, Paris, 2013, pp. 247-256.

[28] J. Ramirez-Nunez, J.A., Antonino-Daviu, J., Climente-Alarcon, V., Quijano-Lopez, A., Razik, H., Osornio-Rios, R.A., de Jesus Romero-Troncoso, R., "Evaluation of the detectability of electromechanical faults in induction motors via transient analysis of the stray flux". *IEEE Transactions on Industry Applications*, 2018.

[29] C. Jiang, S. Li and T. G. Habetler, "A review of condition monitoring of induction motors based on stray flux," *2017 IEEE Energy Conversion Congress and Exposition (ECCE)*, Cincinnati, OH, 2017, pp. 5424-5430.

[30] M. Jeong, J. Yun, Y. Park, S. B. Lee and K. Gyftakis, "Off-line flux injection test probe for screening defective rotors in squirrel cage induction machines," 2017 IEEE 11th International Symposium on Diagnostics for Electrical Machines, Power Electronics and Drives (SDEMPED), Tinos, 2017, pp. 233-239.

[31] F. Vedreno-Santos, M. Riera-Guasp, H. Henao, M. Pineda-Sanchez, and R. Puche-Panadero, "Diagnosis of rotor and stator asymmetries in wound rotor induction machines under nonstationary operation through the instantaneous frequency," *IEEE Trans. Ind. Electron.*, vol. 61, no. 9, pp. 4947–4959, Sep. 2014.

[32] A. Bellini, C. Concari, G. Franceschini, C. Tassoni, A. Toscani, "Vibrations currents and stray flux signals to asses induction motors rotor conditions", *IECON 2006 — 32nd Annual Conference on IEEE Industrial Electronics*, pp. 4963-4968, 2006.

[33] M. Riera-Guasp, J. A. Antonino-Daviu, M. Pineda-Sanchez, R. PuchePanadero, and J. Perez-Cruz, "A General Approach for the Transient Detection of Slip-Dependent Fault Components Based on the Discrete Wavelet Transform," *IEEE Trans. Ind. Electron.*, vol. 55, pp. 4167- 4180, 2008.

[34] J. A. Antonino-Daviu M. Riera-Guasp, J. R. Folch, and M. Pilar Molina Palomares, "Validation of a new method for the diagnosis of rotor bar failures via wavelet transform in industrial induction machines," *IEEE Trans. Ind. Appl.,* vol. 42, pp. 990-996, 2006.

F.Vedreño-Sanchez, *"Diagnosis of electric induction machines in non-stationary regimes working in randomly changing conditions"*, Ph.D. Thesis. Universitat Politecnica de Valencia, 2013.